Supplementary Materials

PneuNet Actuators Design: Trade-offs between Deformation, Force, and Resistance to Buckling

Zeinab Awada[1], Yassine Haddab[1], Marc Gouttefarde[1],

[1]LIRMM, Univ Montpellier, CNRS, Montpellier, France.

This article serves as supplementary material to the paper entitled "PneuNet Actuators Design: Trade-offs between Deformation, Force, and Resistance to Buckling" submitted to Sensors and Actuators A: Physical, Elsevier.

Section 1 demonstrates the variation of the angular deformation as a function of pressure in configurations 1 and 2, considering changes in the actuator length, chamber aspect ratio, and canal design parameters. Section 2 recalls the tip force model cited in the main paper, while Section 3 presents experimental results on the variation of the tip force with changes in the actuator length, chamber longitudinal thickness, and canal dimensions.

Contents

1 Impact of Design Parameters on the Angular Deformation

The change in the angular deformation $\Delta\theta$ in configurations 1 and 2 is studied with respect to the length of the actuator l, the chamber aspect ratio r, the height t_1 and width t_2 of the canal, as well as the vertical t_v and horizontal t_h thicknesses of the silicon around the canal.

The length of the actuator l was increased from 71 mm to 95 mm and the angular deformation of each actuator is plotted as a function of pressure for configurations 1 and 2 in Fig. S1a and Fig. S2a, respectively. The same trend is seen in both configurations: $\Delta\theta$ increases when l decreases. Although angular deformation models suggest that $\Delta\theta$ is proportional to l [2,3], the present results do not reflect this because our actuators lack a strain-limiting layer, which is assumed in the previously cited models. Since the flexural rigidity of the actuator is inversely proportional to l^2 [4], $\Delta\theta$ increases with a decrease in l, corresponding to the results in Fig. S1a and Fig. S2b.

To study the impact of the chamber aspect ratio r on the angular deformation, chambers with narrow, square, and wide shapes are considered. Therefore, r was varied between 0.625 and 1.6. Except for a slight superiority for the actuator with $r = 1$, the other actuators in configuration 2 exhibit very similar $\Delta\theta$ values, with a maximum average difference of less than 10%. On the other hand, more discrepancy is observed in configuration 1, where the narrow actuator ($r = 0.625$) has the lowest angular deformation and the square-shaped actuator ($r = 1$) has the highest. As reported in the main paper, these results confirm that a square chamber actuator yields the largest angular deformation.

The impact of the canal height t_1 and width t_2 on $\Delta\theta$ are given in Fig. S1(c)-(d) and Fig. S2(c)-(d). In both configurations, $\Delta\theta$ reaches its maximum for $t_1 = 4$ mm, while it continuously increases as t_2 increases. These results are explained by calculating the ratio $\frac{e_t A_t}{I_t}$ as a function of t_1 and t_2. This ratio exhibits a parabolic relationship with both parameters, peaking for t_1 before reaching its peak for t_2.

Moreover, the vertical thickness of the silicone around the canal t_v is increased from 2 mm to 5 mm. Except for $t_v = 5$ mm which shows in configuration 1 an angular deformation 15% lower than the other actuators, t_v shows minimal impact on $\Delta\theta$ in both configurations.

Similarly, increasing the horizontal thickness of the silicone around the canal t_h led to a maximum difference of 15% in $\Delta\theta$ in configurations 1 and 2 as shown in Fig. S1f and Fig. S2f. This difference can be reasonably attributed to fabrication and/or experimental inaccuracies, thereby indicating a negligible impact of t_h on $\Delta\theta$.

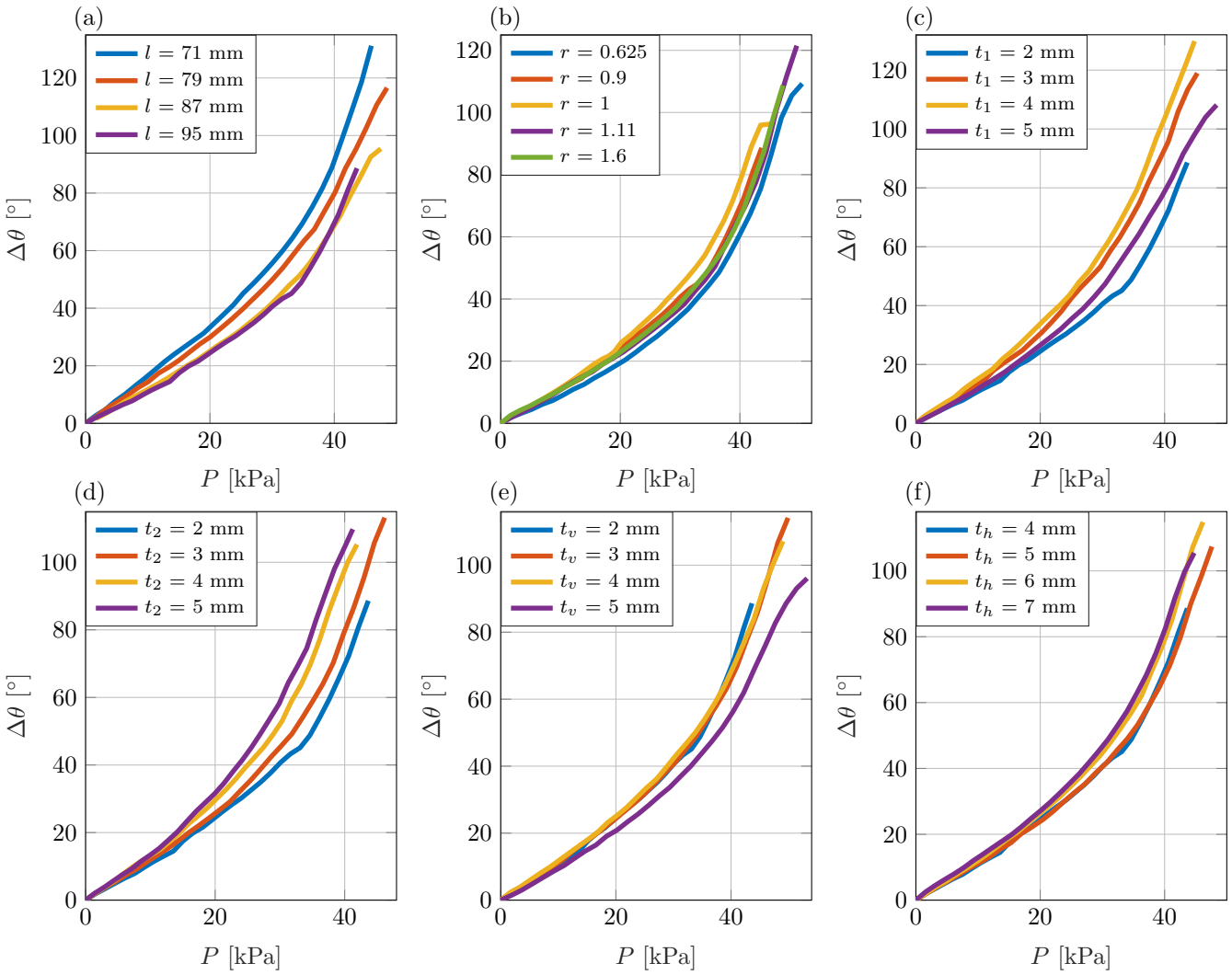

Figure S1: Variation of the angular deformation $\Delta\theta$ as a function of pressure P for different design parameters in configuration 1.

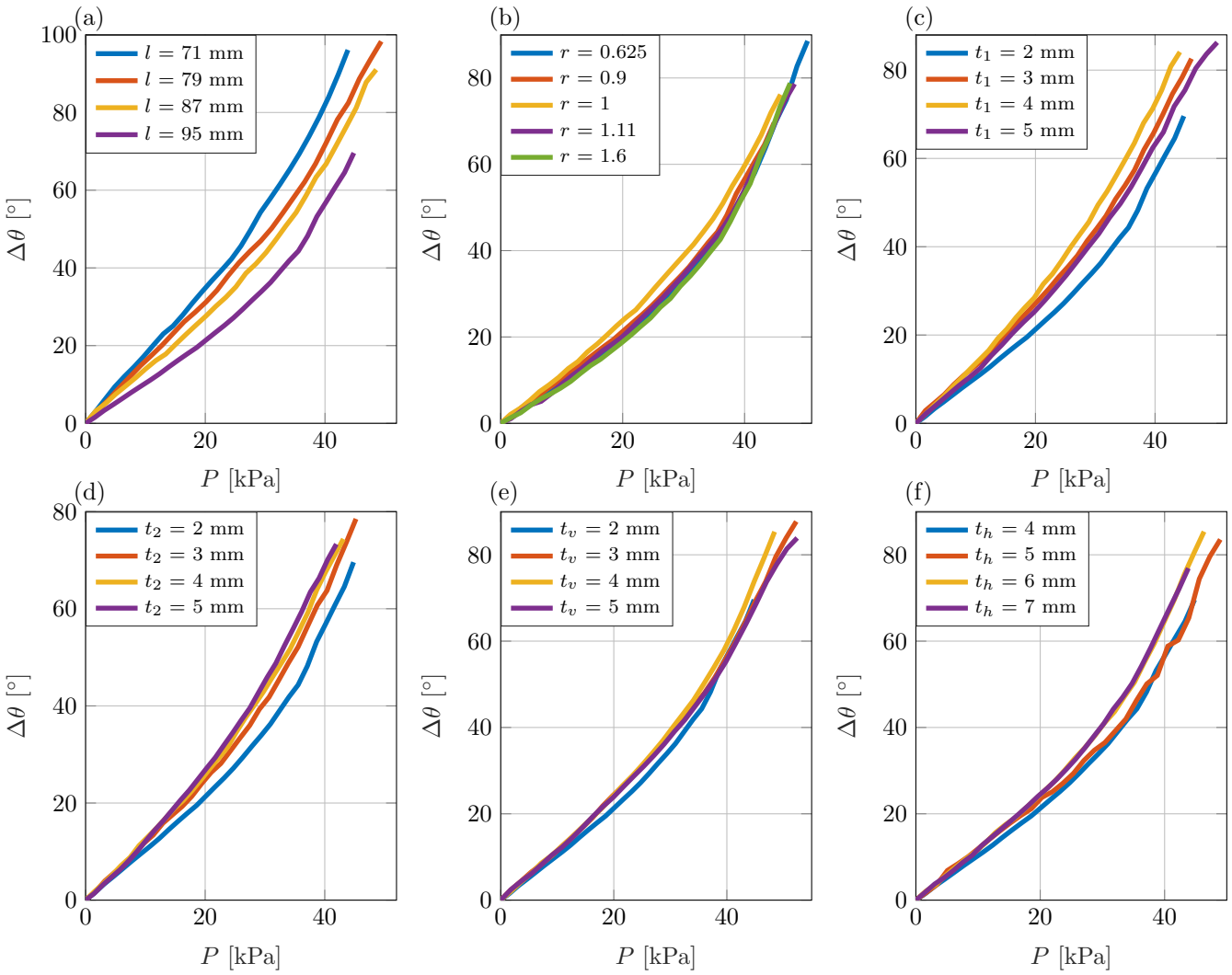

Figure S2: Variation of the angular deformation $\Delta\theta$ as a function of pressure P for different design parameters in configuration 2.

2 Tip Force Model

The modeling of the tip force F_t in a PneuNet actuator with an inextensible layer is discussed in [1] and is given by the following equation

$$F_t = \frac{F_c d_{mb}}{l_2 + 2t_{ch} + \frac{t_s}{2}} \cos(\alpha) \tag{S1}$$

In this equation, α is the angle between the tip force F_t and the deflection of the silicone base, F_c is the contact force between the last two chambers, l_2 is the length of the chamber, t_{ch} is the longitudinal thickness of the chamber, and t_s is the space between the chambers.

3 Impact of Design Parameters on the Tip Force

Eq. S1 suggests that F_t decreases as the chamber longitudinal thickness t_{ch} increases and as the length of the chamber l_2 (and consequently the total length of the actuator l) increases. To the best of our knowledge, no experimental validation has been conducted to test these two suggestions. To address this gap, t_{ch} was varied between 1.5 mm and 4 mm, while l was varied between 71 mm and 95 mm.

Fig. S3a-b demonstrates that the trends suggested by Eq. S1 hold true. Specifically, the tip force for the actuator with $t_{ch} = 4$ mm is, on average, 60% less than that of the actuator with $t_{ch} = 1.5$ mm. Furthermore, as l decreases, an increase in F_t is observed. For $l = 79$ mm and $l = 71$ mm, F_t is, on average, 22% and 40% higher, respectively, than that of $l = 95$ mm.

Moreover, neither Eq. S1 nor previous studies provide any insight into how F_t is impacted by the height t_1 and width t_2 of the connecting canal of the PneuNet actuator. Therefore, both design parameters were varied between 2 mm and 5 mm, and the corresponding tip forces of each actuator are shown in Fig. S3c-d. In both cases, F_t increases with an increase in t_1 and t_2. The highest recorded increase is 24% compared to the reference PneuNet actuator ($t_1 = 2$ mm and $t_2 = 2$ mm). This increase is attributed to the enlargement of the canal airflow area, which enhances the force application.

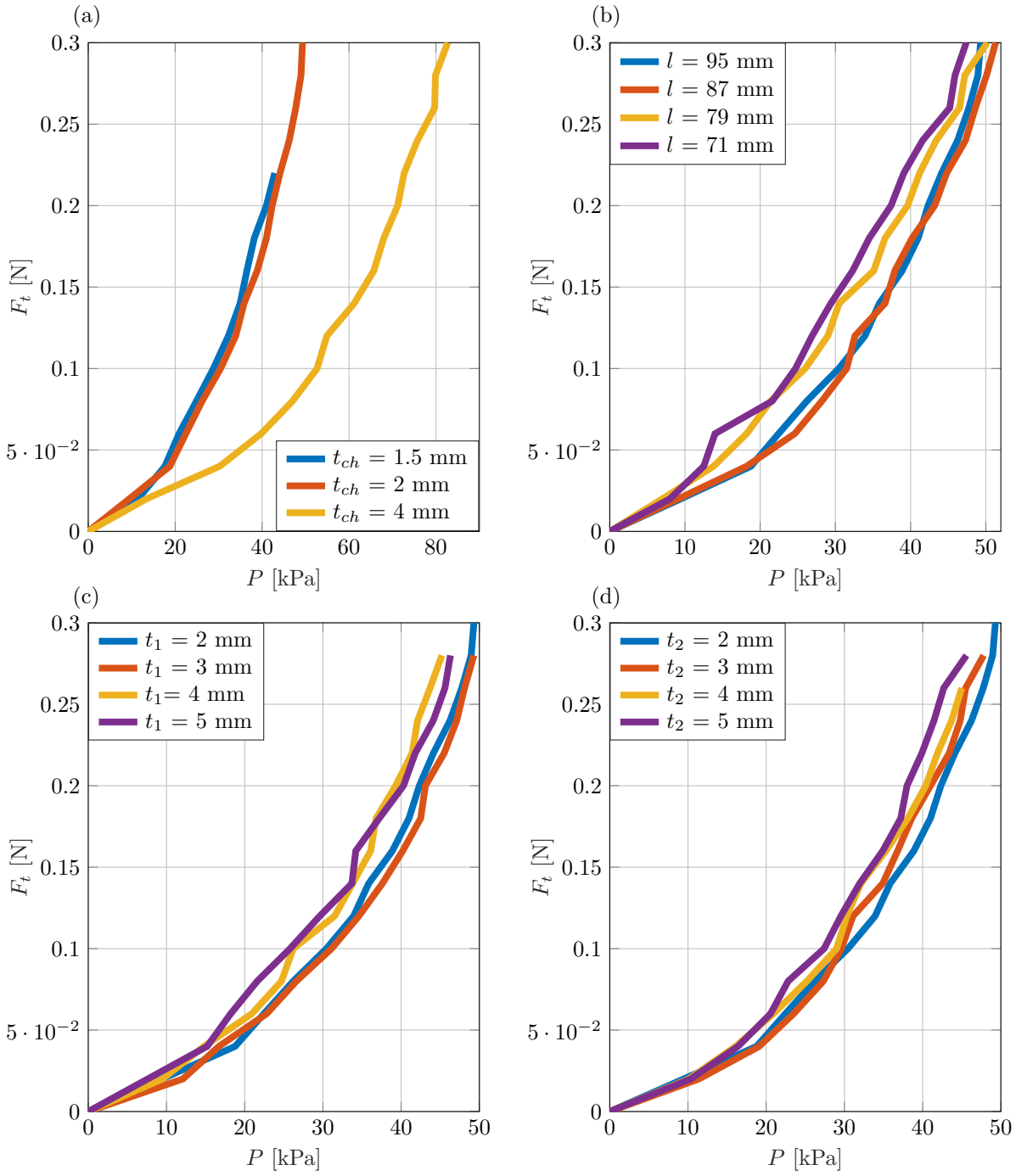

Figure S3: Variation of the tip force F_t as a function of pressure P for different values of (a) t_{ch}, (b) l, (c) t_1, and (d) t_2.

References

[1] S. Nikolov et al., "Combined Analytical-FE Modeling of the Deformation Mechanisms and Forces in Soft PneuNets Bending Actuators," *2022 IEEE International Conference on Manipulation, Manufacturing and Measurement on the Nanoscale (3M-NANO)*, Tianjin, China, 2022, pp. 301-306.

[2] G. Zhong, W. Dou, X. Zhang, and H. Yi, "Bending analysis and contact force modeling of soft pneumatic actuators with pleated structures," *International Journal of Mechanical Sciences*, vol. 193, p. 106150, Mar. 2021.

[3] Z. Liu, F. Wang, S. Liu, Y. Tian and D. Zhang, "Modeling and Analysis of Soft Pneumatic Network Bending Actuators," in *IEEE/ASME Transactions on Mechatronics*, vol. 26, no. 4, pp. 2195-2203, Aug. 2021.

[4] G. Alici, T. Canty, R. Mutlu, W. Hu, and V. Sencadas. "Modeling and Experimental Evaluation of Bending Behavior of Soft Pneumatic Actuators Made of Discrete Actuation Chambers," *Soft Robotics*, vol. 5, no .1, pp. 24–35, Feb. 2018.